CORRELATION FILTERING OF MODAL DYNAMICS USING THE LAPLACE WAVELET

Lawrence C. Freudinger, Rick Lind and Martin J. Brenner

NASA Dryden Flight Research Center
Edwards, CA 93523-0273

Abstract

Wavelet analysis allows processing of transient response data commonly encountered in vibration health monitoring tasks such as aircraft flutter testing. The Laplace wavelet is formulated as an impulse response of a single mode system to be similar to data features commonly encountered in these health monitoring tasks. A correlation filtering approach is introduced using the Laplace wavelet to decompose a signal into impulse responses of single mode subsystems. Applications using responses from flutter testing of aeroelastic systems demonstrate modal parameters and stability estimates can be estimated by correlation filtering free decay data with a set of Laplace wavelets.

1. Introduction

Experimental modal analysis techniques are often difficult to implement for on-line vibration health monitoring tasks due to prohibitive time and cost requirements along with inherent limitations in the formulations. Rapid analysis of transient responses from multiple mode systems for which no accurate plant model exists is especially problematic. Such analysis is required for safe and efficient health monitoring during flight flutter testing of aircraft for which the modal parameters can arbitrarily change with flight condition, loading, configuration and structural variations.

Modal filtering and parameter estimation techniques have been studied in the context of flutter testing and indicate improved signal analysis methods can increase efficiency [7, 13]. Modal filtering is a promising approach because sensor arrays can be condensed and information about stability can be directly obtained but current filters are not robustly adaptive to variations from the aircraft dynamics [12]. Parameter estimation methods can adapt to variations but are often unreliable with low signal-to-noise ratios.

Wavelet analysis is a signal processing technique well suited to flutter testing. This analysis operates on small time windows of the signal using finite duration waveforms called wavelets [14]. This localized approach processes nonstationary data due to transient responses or time-varying dynamics. Modal properties are interpreted from dominant features in the signals.

There has been recent work in applying wavelets to analysis of flight flutter test data [2]. In this other work, measured data are represented in the time-frequency plane which allows desired excitation and response features to be easily extracted using a masking or denoising algorithm. Parameter estimation algorithms can use the mask filtered data effectively and identify linear models. A class of wavelets has been developed for analysis of dynamical systems which generates information similar to modal filtering [8]. Two members of this class, denoted the Haley wavelet and Laplace wavelet, are formulated to resemble responses of single mode systems. A matching pursuit algorithm decomposes a response into a sum of modal responses correlating to the wavelets [9]. This algorithm is effective for analyzing flutter response data but the excessive computational cost prohibits a reasonable on-line implementation.

This paper introduces a correlation filtering approach for modal analysis based on a modified version of the Laplace wavelet. This procedure uses vector inner products between a time history and a set of Laplace wavelets as a measure of correlation between the data and a range of modal dynamics described by the wavelets. Local maxima in the correlations are used to indicate which Laplace wavelet parameters may be closest to modal parameters of the system being observed. This filtering is related to modal filtering and parameter estimation methods because a signal is interpreted as responses from subsystems with determined modal properties. Correlation filtering augments existing tools for several reasons. Correlation filtering adapts to modeling errors and retains some level of performance with realistic noisy flight data. The proposed approach may enhance interpretation of modally filtered sensor arrays in the presence of noise and errors in the modal filter, and is acceptable from a computational standpoint for on-line implementation.

This paper presents the Laplace wavelet correlation algorithm and applies it to numerical and experimental data relevant to flight flutter testing of aircraft.

2. The Laplace Wavelet

The Laplace wavelet, ψ, is a complex, analytic, single-sided damped exponential.

$$\psi(\omega,\zeta,\tau,t) = \psi_\gamma(t) = \begin{cases} Ae^{-\frac{\zeta}{\sqrt{1-\zeta^2}}\omega(t-\tau)}e^{-j\omega(t-\tau)} & : t \in [\tau, \tau+T] \\ 0 & : \text{else} \end{cases}$$

The parameter vector $\gamma = \{\omega, \zeta, \tau\}$ determines the wavelet properties. These parameters are related to modal dynamic properties and are denoted frequency $\omega \in \mathcal{R}_+$, viscous damping ratio $\zeta \in [0,1) \subset \mathcal{R}_+$, and time index $\tau \in \mathcal{R}$. The coefficient A is an arbitrary scaling factor, used here to scale each wavelet to unity norm. The range T ensures the wavelet is compactly supported and has nonzero finite length but the parameter T is generally not explicitly expressed.

This function is called a Laplace wavelet to emphasize its derivation is related to the Laplace transform. In particular, the Laplace wavelet has a strong similarity to the inverse Laplace transform of the transfer function for an underdamped second order system. An example Laplace wavelet is shown in Figure 1.

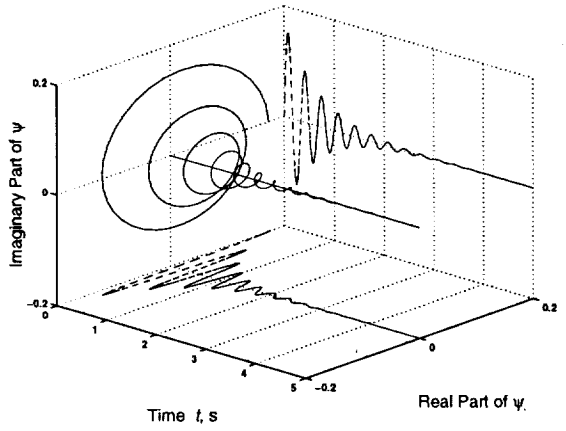

Figure 1: Real and Imaginary Components of the Laplace Wavelet for Parameters $\omega = 3$ *Hz*, $\zeta = 0.08$, $\tau = 0$ and Support Range $T = 5$ *s*

Figure 1 also shows the projections of ψ_γ onto the real and imaginary planes. These projections graphically demonstrate the relationship between the wavelet and an impulse response of a single mode system. The Laplace wavelet has real and imaginary parts which are 90^o out of phase. In a manner similar to the Fourier transform, a complex wavelet is required to properly handle phase differences between the wavelet and the signal. A wavelet could be derived with only a real part to match physical data which is typically real. However, using both parts ensures a smoothness and continuity of the wavelet transform.

It should be noted that the Laplace wavelet is generated by considering features anticipated in mechanical system responses. Additional properties, such as orthogonality, often associated with wavelets derived from formal filter theory are not associated with the Laplace wavelet [14]. The absence of these properties limits the usefulness of the Laplace wavelet since some operations, such as rapid signal reconstruction, are not straightforward. This wavelet is introduced in a limited capacity for situations requiring rapid assessment of modal dynamics from free response measurements.

3. A Laplace Wavelet Dictionary

The analysis of response data from dynamical systems often uses assumptions of linearity such that the system response should be a linear combination of subsystem responses [6]. These subsystems are second order single degree of freedom systems in the case of modal analysis. Signal decomposition of the response into the subsystem responses for steady state data can be accomplished via Fourier transforms which use a basis of infinite length sinusoids of varying frequencies.

Transient response data is difficult to effectively decompose even for linear systems since the system response is composed of subsystem responses with time-varying magnitudes. The basis of infinitely long sinusoids used by the Fourier transform is not ideal for this nonstationary data. Wavelets may be used for signal decomposition of transient response data since they inherently allow time-varying magnitudes of the subsystem responses.

The concept of a dictionary is introduced to describe a set of wavelets used for signal decomposition [14]. This dictionary is distinguished from a basis since the response of any dynamical system may not necessarily be expressed as a linear combination of the finite number of entries in the dictionary. The dictionary approximates a basis assuming the responses to be analyzed are similar in nature to the Laplace wavelets. The dictionary is basically a database of waveforms.

A finite set of wavelet parameters is used to generate the dictionary. A discrete gridding of the parameter

space results in sets $\Omega, \mathcal{Z}$ and $\mathcal{T}$.

$$\begin{aligned} \Omega &= \{\omega_1, \omega_2, \ldots, \omega_p\} \subset \mathcal{R}_+ \\ \mathcal{Z} &= \{\zeta_1, \zeta_2, \ldots, \zeta_q\} \subset \mathcal{R}_+ \cap [0,1) \\ \mathcal{T} &= \{\tau_1, \tau_2, \ldots, \tau_r\} \subset \mathcal{R} \end{aligned}$$

The dictionary, Ψ, is defined for the set of Laplace wavelets whose parameters are contained in these sets as denoted by $\gamma \in \Gamma = \Omega \times \mathcal{Z} \times \mathcal{T}$.

$$\Psi = \{\psi(\omega, \zeta, \tau, t) \ : \ \omega \in \Omega, \zeta \in \mathcal{Z}, \tau \in \mathcal{T}\}$$

4. Correlation Filtering

An inner product operation measures the correlation between signals. Correlating a signal with a Laplace wavelet measures similarity between frequency and damping properties of the wavelet, ψ_γ, and the system which generated the signal $f(t)$. The inner product (or *dot* product or *scalar* product) for finite length vectors can be expressed mathematically several ways, *e.g.*

$$< \psi_\gamma(t), f(t) >= \|\psi_\gamma\|_2 \|f\|_2 \cos(\theta) = f(t)^* \psi_\gamma(t)$$

A correlation coefficient, $\kappa_\gamma \in \mathcal{R}$, is defined to quantify the degree of correlation between the wavelet and a time signal. This correlation coefficient considers the angle θ between the vectors with the maximum correlation occurring for vectors whose angle is $\theta = 0$.

$$\kappa_\gamma = \sqrt{2} \frac{|< \psi_\gamma, f(t) >|}{\|\psi_\gamma\|_2 \|f\|_2}$$

κ_γ is a matrix whose dimensions are determined by the parameter vectors of $\{\omega, \zeta, \tau\}$. A useful correlation coefficient $\kappa(\tau)$ is defined for on-line modal analysis to correlate frequency and damping at each time value. Peaks of the surface plot κ_γ for a given τ relate the wavelets with the strongest correlation to the data. Define $\kappa(\tau)$ as the peak values of κ_γ at each τ and define $\overline{\omega}$ and $\overline{\zeta}$ as the parameters of the Laplace wavelet associated with the peak correlation.

$$\kappa(\tau) = \max_{\substack{\omega \in \Omega \\ \zeta \in \mathcal{Z}}} \kappa_\gamma = \kappa_{\{\overline{\omega}, \overline{\zeta}, \tau\}}$$

A normalizing factor of $\sqrt{2}$ allows $\kappa(\tau) = 1$ when the signal in some time interval T is a linear combination of the real and imaginary components of a particular wavelet. The formulation of $\kappa(\tau)$ searches for a maximum value across values of ω and ζ. This search can use subsets of Ω and $\mathcal{Z}$ to find local maxima and compute a κ vector at each time index. The subset searching is analogous to finding multiple peaks of interest on a frequency spectrum plot, with the added variables of damping and time.

The support range T is not explicitly used to define κ but it can greatly affect the computed value. Small T may increase κ for signals not strongly correlated while large T may decrease κ to the noise floor even for signals which are strongly correlated. Thus, T can not be chosen arbitrarily. Knowledge of crest factors, signal-to-noise ratios, and effective decay rates observed in the data can all be used in guiding the choice of T.

A correlation filter approach computes the κ vector for a response signal. The dampings $\overline{\zeta}$ and frequencies $\overline{\omega}$ associated with peak κ values indicate the modal properties of the system which generated the data. This filter acts as a transform from the time domain to a modal parameter, or stability, domain. This stability estimate should be representative of the modal properties of the system if the data represent a linear time invariant system in free decay.

5. Application : Test Signal

An application of correlation filtering using Laplace wavelets on a test signal with known properties is instructive to demonstrate the method. Consider the test signal $f(t)$.

$$f(t) = e^{-\frac{\zeta_o}{\sqrt{1-\zeta_o^2}}\omega_o(t-t_o)} \sin(\omega_o(t-t_o)) + .01n(t)$$

$$\text{with } f(t) = .01n(t) \text{ for } t < t_o$$

$f(t)$ is a real exponentially damped sinusoidal signal corresponding to an impulse response of a single mode system. The dynamical properties of that system, ζ_o and ω_o, are given in Table 1 along with the time index at which the impulse is applied. The signal $n(t)$ is a unity bounded random noise weighted by 0.01. The signal sampling rate is 200 *Hz*.

ζ_o	.04
ω_o	10 *Hz*
t_o	0 *s*

Table 1: Properties of Test Signal

A dictionary Ψ of Laplace wavelets is used for analyzing this test signal. The grid of wavelet parameters is nonuniform to provide higher resolution at lower damping values. Using MATLAB™ syntax, define the sets of parameters such that $\Gamma = \Omega \times \mathcal{Z} \times \mathcal{T}$.

$$\begin{aligned} \Omega &= \{5 : 0.5 : 20\} \\ \mathcal{Z} &= \{\{0.005 : 0.005 : 0.2\} \{0.3 : 0.1 : 0.9\}\} \\ \mathcal{T} &= \{-5 : 0.1 : 5\} \end{aligned}$$

At each value of $\tau \in \mathcal{T}$ a matrix of correlation coefficients κ_γ is computed. The dimension of this matrix is determined by the sizes $\dim(\Omega) = 31$ and

$\dim(\mathcal{Z}) = 47$. Also, the support of the wavelet is $T = 4\ s$ indicating the vectors used for each inner product calculation of κ_γ have 800 elements since the sampling rate is 200 Hz. Thus, 1457 inner products with vector lengths of 800 must be computed to determine $\kappa(\tau)$ for each of the 151 starting time values $\tau \in \mathcal{T}$. The computational cost of correlation filtering is clearly greater than the cost of Fast Fourier transforms. This computational burden is offset by the information gained from time-localized analysis away from the $j\omega$ axis at multiple values of ζ.

Figure 2 presents the information obtained by correlation filtering of the test signal $f(t)$ with the Laplace wavelet dictionary Ψ.

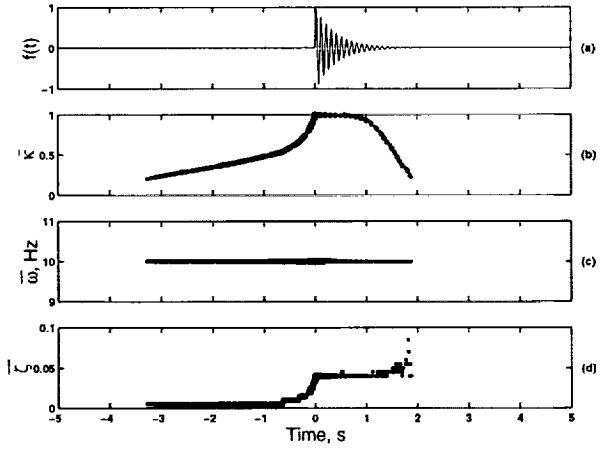

Figure 2: Correlation Filtering of the Test Signal with the Laplace Wavelet Dictionary Ψ : Test Signal $f(t)$ (a), Peak Correlation Coefficient $\kappa(\tau)$ (b), Wavelet Frequency $\overline{\omega}$ Associated with Peak κ (c), Wavelet Damping $\overline{\zeta}$ Associated with Peak κ (d)

Figure 2a presents the test signal $f(t)$ while subplot Figure 2b presents the correlation coefficient $\kappa(\tau)$ for each value of $\tau \in \mathcal{T}$. A threshold $\kappa(\tau) > 0.3$ is applied such that information is presented only from values of τ at which a significant correlation level is obtained.

The values of $\kappa(\tau)$ are near unity starting at the onset of the impulse and lasting for approximately 0.8 s. These high correlation levels indicate some wavelet $\psi \in \Psi$ in the dictionary has parameters that closely match the dynamics which dominate the response during these times.

Figures 2c and 2d present modal information obtained from the correlation filtering. This information relates to the frequency and damping parameters of the Laplace wavelet which had the largest correlation at time τ. The frequency $\overline{\omega} = 10\ Hz$ is constant throughout the time range at which the correlation coefficient is greater than the minimum threshold. This wavelet frequency is the dictionary entry nearest to (same as) the frequency ω_o of the test signal given in Table 1.

The damping $\overline{\zeta}$ is time-varying with initial dampings low and increasing until the correct value of $\overline{\zeta} = 0.04$ is obtained after $\tau \geq t_o$. This behavior is indicative of the inner product function in the correlation filtering which begins to be noticeable when the wavelet support overlaps the nonzero component of the signal. Low damped wavelets are nonzero for longer durations and thus overlap the signal sooner. This explains the artificially low values prior to $t = 0s$. Highly damped wavelets decay rapidly which means their effective support is smaller. Adding noise to the signal reduces κ for the correct damping value and increase κ for wavelets with smaller effective support. This explains artificially high damping estimates for low signal-to-noise ratios. When the support, or analysis window, is observing the system at $t \geq t_o$ in free decay without excessive noise, the estimated damping value is correct.

$\kappa(\tau)$ is obtained by determining local maxima of the matrix κ_γ which considers the correlation coefficients for all $\omega \in \Omega$ and $\zeta \in \mathcal{Z}$. A surface plot showing the value of the correlation coefficients in this matrix at the onset of the impulse, $\tau = t_o$, is shown in Figure 3.

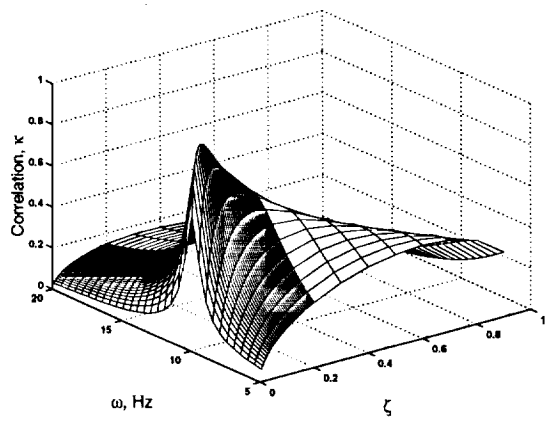

Figure 3: Surface Map of Correlation Coefficient κ_γ Obtained from Correlation Filtering of the Test Signal with a Subset of the Laplace Wavelet Dictionary Ψ at $\tau = t_o = 0\ s$

The peak in Figure 3 at frequency $\overline{\omega} = 10\ Hz$ and damping $\overline{\zeta} = 0.04$, also shown in Figure 2c and 2d, matches the signal properties given in Table 1. This plot demonstrates an effect of using the wavelet dictionary since the peak would be a narrow spike if the dictionary were comprised of orthogonal basis elements.

The surface gradient near the peak in Figure 3 provides insight into analysis of the wavelet parameters in Figures 2c and 2d. That analysis notes the frequency associated with the peak correlation remains constant while the damping is time-varying. The gradient of the surface at ω_o, ζ_o in Figure 3 in the fre-

quency direction is steep but is relatively shallow as damping is changed. This surface and the analysis of Figure 2 suggest that correlation filtering is similar to other techniques in regard to being more accurate in frequency than in damping.

These features of $\kappa(\tau)$ presented in Figure 2 and Figure 3 demonstrate the information that may be obtained from correlation filtering using Laplace wavelets. Monitoring the value of κ indicates the occurrence of impulsive events. The time period at which the decaying response to that impulse is significant can be obtained by monitoring the length of time for which κ retains a high value near 1. Also, the wavelet parameters associated with the peaks of $\kappa(\tau)$ indicate the dynamic properties of the subsystem(s) dominating the response. Thus, correlation filtering using Laplace wavelets, despite the lack of an orthonormal basis or a parameter estimation algorithm, can be seen as a type of modal filtering.

6. Application : Flight Test Data

Application to actual aircraft data is required to evaluate Laplace wavelet correlation filtering for use in a flight test environment. Consider the DAST aircraft (Drones for Aerodynamic and Structural Testing), a remotely piloted research drone which encountered explosive flutter in June 1980 [5].

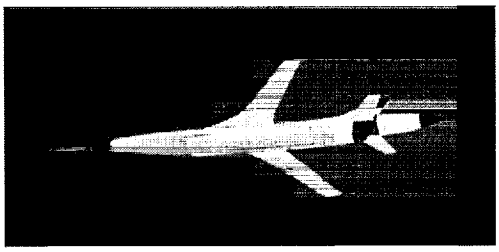

Figure 4: NASA DAST vehicle in flight

Consider the last forty seconds of wingtip acceleration response prior to the onset of flutter. The aircraft was flying at 15,000 *ft* and Mach number varied between approximately 0.80 and 0.825. Pulse responses were being induced during this time frame via symmetric aileron pulses. A closed-loop flutter suppression control system was engaged. Due to an implementation error, the controller could not maintain a stable system, and the flutter instability was encountered. The response data was correlated with a Laplace dictionary of support $T = 2s$ and with the following parameters:

$$\begin{aligned} \Omega &= \{10 : 0.25 : 30\} \\ \mathcal{Z} &= \{0 : 0.003 : 0.063\} \end{aligned}$$

The sampling rate for this data is 500 *Hz*. Starting time indices τ are data dependent and correspond to local maxima in the time domain signal $y(t)$. This selection is not optimum in all cases but corresponds to an emphasis on transient excursions. The resulting correlation map is presented in Figure 5.

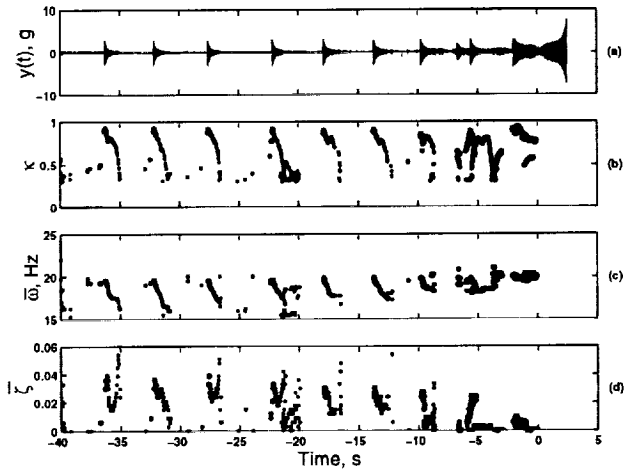

Figure 5: Correlation Filtering of the DAST Data with the Laplace Wavelet Dictionary: Left Wingtip Acceleration (a), Peak Correlation Values $\kappa(\tau) > 0.3$ (b), Wavelet Frequencies Associated with Peak Correlations (c), Corresponding Wavelet Damping Values (d)

Figure 5a presents the acceleration response of the left wingtip while Figures 5b, 5c, and 5d present the peak correlation, frequency, and damping values as a function of time. A threshold $\kappa(\tau) > 0.3$ is applied to avoid clutter on the plot without discarding interesting information. Symbol size is proportional to inner product magnitude $|< \psi_\gamma, y(t) >|$ to provide information on the plot related to the time history magnitude.

From the frequency values a trend is visible. Beginning at $t = -36s$, each symmetric aileron pulse response correlates first at a high frequency (approximately 20 *Hz*) and transitions to a lower frequency, as low as 15 *Hz*. The frequency spread decreases as the flutter condition is approached. The lower frequency changes while the upper one is mostly constant, resulting in a flutter frequency at $t = 0s$ of approximately 19.7 *Hz*. This corresponds with predicted and observed characteristics as reported in the literature [10].

Describing the frequency trend is open to interpretation. The correlation values κ decrease away from the pulse onset, indicating lower confidence in those lower frequency estimates. However, the fact that this lower frequency limit trends into the flutter frequency suggests that it can not be ignored. Note that 2 other modes, antisymmetric wing bending and vertical fuselage bending, are active near 16 *Hz*. The antisymmetric bending mode is also predicted to have a transonic

flutter mechanism but the symmetric mode had the lower flutter speed [1, 5]. To complicate the analysis further, note that the symmetric bending mode would shift toward 16 *Hz* if the flutter suppression system were disengaged.

The amplitude-dependent frequency estimates for each pulse is characteristic of a hardening spring. Nonlinearities could have aerodynamic, structural, or control system origins. However, a hardening spring transitions to a linear system at small amplitudes, which should be accompanied by an increase in correlation κ for small amplitudes. This is not clearly observed here, although there is some indication that frequency locks onto a constant at small amplitudes. What can be said for certain is that the pulses do not look like responses of a system. What is still open to scrutiny is whether the estimated frequencies represent actual physical phenomena or show limitations of the approach when applied to multimode systems in the presence of noise.

The damping correlations in Figure 5d also show interesting characteristics. For the 4 pulse responses between $t = -37s$ and $t = -20s$, the decreasing frequencies are matched with decreasing damping values. Three of these 4 responses are further followed by a sharp increase in damping, forming a "V" pattern. Ignoring the frequency analysis for the moment, this could indicate a nonviscous or more complicated damping mechanism or it could merely be the effect of the decreasing signal-to-noise ratio. The increasing damping values due to noise was demonstrated in Figure 2. In any case, the pulse response data do not represent clearly linear time invariant modal dynamics.

The correlation coefficients κ presented in Figure 5b offer a quantitative measure of confidence in each frequency and damping estimate. These κ values are higher near 20 *Hz* at the beginning of the pulse and trend downward rather quickly. Reduced confidence for frequency and damping estimates is justified where the correlation coefficient is relatively low. In particular, the pulses with the aforementioned "V" pattern are revealed to be similar to the other pulses when the estimates are filtered further using a higher threshold value of κ. This filtered result is shown in Figure 6 for $\kappa \geq 0.8$.

Classical flutter testing trend analysis requires grouping correlations for a given pulse into an average value. The results from performing this operation by inspection of Figure 6 for both frequency and damping is presented in Table 2.

As can be seen in both Figure 6 and Table 2, the average frequency and damping values show a roughly steady trend until the impulse at $t = -13s$ at which time the dominant frequency edges up slightly by 0.5 *Hz* and the damping trend accelerates toward zero. From $t = -9s$ and later a progressive increase in residual dynamics observed in Figure 6a indicates the arrival of the stability boundary. The correlations do identify this, but the choice of starting indices were selected to emphasize transient peaks. As the frequency spread converges to a single frequency, the damping values converge to zero. These estimates agree with previous parameter estimation results [1].

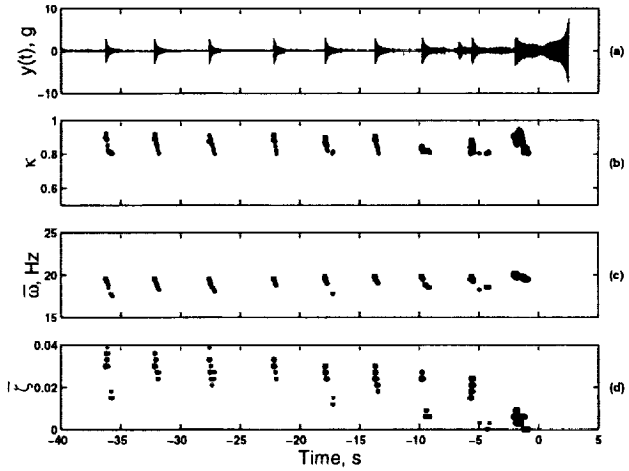

Figure 6: Correlation Filtering of the DAST Data with the Laplace Wavelet Dictionary: Left Wingtip Acceleration (a), Peak Correlation Values $\kappa(\tau) > 0.8$ (b), Wavelet Frequencies Associated with Peak Correlations (c), Corresponding Wavelet Damping Values (d)

t, s	$\bar{\zeta}$	$\bar{\omega}, Hz$
-36	0.035	18.25
-32	0.030	18.75
-27	0.027	19.0
-22	0.026	19.0
-17	0.025	19.2
-13	0.022	19.0
-9	0.025/0.009	19.5/18.5
-5	0.018/0.0	19.5/18.5
-2	0.005	19.7
-1	0.000	19.7

Table 2: Frequency and Damping Values of DAST vehicle From Inspecting Laplace Wavelet Correlation Analysis of Flight Data

This analysis demonstrates that frequency and damping estimates provided by Laplace wavelet analysis are a diagnostic tool useful for free decay analysis because it provides time varying estimates at arbitrary resolutions, which are not available from Fourier or traditional linear estimation techniques. This information

is particularly useful in cases such as the DAST where pulse responses of closed loop systems are observed specifically with the intent of tracking modal dynamics in the time domain. While it may not be possible to identify the source of nonstationary or nonlinear behavior, non-constant $\overline{\omega}$ and $\overline{\zeta}$ implies that a signal is not behaving like a linear time invariant second-order viscously damped system. This knowledge directly impacts confidence one can place on damping trends obtained from traditional approaches.

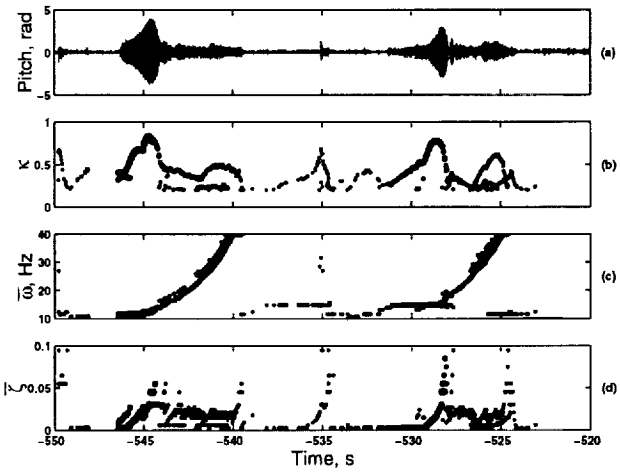

Figure 7: Correlation Filtering of DAST Sweep Data with the Laplace Wavelet Dictionary: Left Wingtip Acceleration (a), Peak Correlation Values $\kappa(\tau)$ (b), Wavelet Frequencies Associated with Peak Correlations (c), Wavelet Damping Associated with Peak Correlations (d)

The knowledge added by Laplace wavelets when interpreting forced response data is less clear. Consider a typical pair of sinusoidal sweeps, symmetric then antisymmetric, for the DAST aircraft at a stable flight condition. The flight condition for this data is 0.7 Mach number, 15000 *ft* and the flutter suppression system is turned off. The left wingtip acceleration is presented in Figure 7 with the Laplace wavelet analysis corresponding to the following parameters.

$$\begin{aligned} \Omega &= \{10 : .8 : 40\} \\ \mathcal{Z} &= \{\{.003 : .003 : .063\}\{.045 : .01 : .1\}\} \end{aligned}$$

The support for this dictionary is $T = 3\ s$ and 500 time domain local maxima were chosen as starting time indices τ. Figure 7a presents the acceleration response being analyzed, while Figures 7c and 7d present the resulting frequency and damping parameters of the Laplace wavelets. A threshold of $\kappa(\tau) > .2$ was used and is presented in Figure 7b.

The frequency information presented in Figure 7c clearly identifies the instantaneous frequency of the excitation as a function of time. The correlation κ increases near resonances visible in the time history. For this particular run, the first sweep is dominated by a 12 *Hz* mode, while the second sweep excites a 15 *Hz* mode. The 15 *Hz* mode is also excited by a pulse applied between the sweeps at $-535s$. These frequencies correspond to the primary symmetric and antisymmetric wing bending modes, respectively. Other modes are indicated but are not discussed here.

Interpreting the damping plot is difficult. The algorithm tracks the forcing frequency, and the damping generally correlates with small but nonzero values. Local maxima occur in the damping trend as the response passes through a resonance, but there is no obvious way to separate reasonable damping values from unreasonable ones. In addition, there is no reason to suggest that any of these damping values for a forced response would be representative of actual system properties.

The analyses of flight data presented here demonstrate the value of Laplace wavelet correlation studies for gaining insight into the dynamics of free decay signals relevant to hazardous flight flutter testing and stability monitoring. This analysis results in estimates of frequency and damping versus time, with a measure of relative confidence in those estimates. For forced response studies, the time-frequency information provided by the Laplace wavelet is more useful than the time-damping information.

7. Application : Nonlinear System

The Laplace wavelet is derived to correlate highly with impulse responses from linear systems. However, correlation filtering with the Laplace wavelet can also be used to analyze responses from nonlinear systems by interpreting frequency and damping parameters as local frequency and decay rate. This filtering can also be used to characterize the modal properties of the linearized dynamics when the system response is relatively close to an equilibrium condition such that the nonlinearity is not strongly excited.

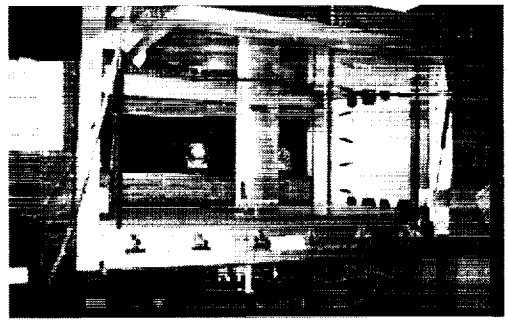

Figure 8: Texas A&M University Aeroelastic Testbed

A nonlinear aeroelastic testbed has been developed at Texas A&M University for flutter research using a prototypical wing section as shown in Figure 8 [11]. Consider the aeroelastic equations of motion for this pitch-plunge system.

$$M\begin{Bmatrix}\ddot{y}\\ \ddot{\alpha}\end{Bmatrix} + C\begin{Bmatrix}\dot{y}\\ \dot{\alpha}\end{Bmatrix} + K\begin{Bmatrix}y\\ \alpha\end{Bmatrix} + \begin{Bmatrix}0\\ k_\alpha\alpha\end{Bmatrix} = \begin{Bmatrix}-F_L\\ F_M\end{Bmatrix}$$

System state y is the plunge position and α is the pitch angle while matrices M, C and K are the structural mass, damping and stiffness matrices. The lift F_L and moment F_M are linear functions of α, $\dot{\alpha}$ and $\dot{y}$ as determined by quasi-steady aerodynamic theory.

Nonlinearities are introduced to the system dynamics through the spring function k_α which is a polynomial function of the pitch angle. This type of nonlinearity is equivalent to a nonlinear stiffness which can induce limit cycle oscillation phenomena [3]. The spring function used in this paper models a hardening spring.

$$k_\alpha = 2.82 - 62.3\alpha + 3709.7\alpha^2 - 24196.0\alpha^3 + 48757\alpha^4$$

A nonlinear flutter mechanism resulting in a bounded limit cycle oscillation occurs at $U = 13.5$ m/s with an amplitude that increases as airspeed increases for the system with this particular k_α [4].

The equations of motion can be linearized around small pitch angles α to compute a 2 mode model. The mode shapes involve both state parameters although one mode is associated mainly with plunge motion while the other mode is associated mainly with pitch motion. The parameters of these modes are given in Table 3 for different airspeeds.

	U=4	U=6	U=8	U=10	U=15.6
ω_y	2.45	2.44	2.41	2.37	2.20
ω_α	1.58	1.62	1.67	1.78	2.07
ζ_y	.079	.081	.084	.089	.177
ζ_α	.054	.055	.055	.054	-.029

Table 3: Predicted Modal Properties of the Linearized Texas A&M University System At Airspeeds U in m/s

A classical flutter instability is encountered for the linearized dynamics at $U = 15.6$ m/s from the two modes coupling with the damping increasing for one mode and decreasing for the other as the natural frequencies coalesce. The limit cycle instability is caused by the nonlinear stiffness so is not predicted with the linearized dynamics.

Laplace wavelet correlation analysis of a simulation of the nonlinear system validates the correlation approach for linearized dynamics. For this analysis, the wavelet parameters are

$$\begin{aligned}\Omega &= \{.5 : .1 : 5\}\\ \mathcal{Z} &= \{\{0 : .005 : .03\}, \{.04 : .01 : .1\}, \{.2, .3\}\}\end{aligned}$$

with the set of starting time indices τ again determined from time domain peak searching. The support of the wavelets is 3 s. Two free decays of the pitch degree of freedom at airspeeds $U = 6, 8$ m/s due to an initial condition of .02 m for plunge and 0^o for pitch angle are shown in Figure 9.

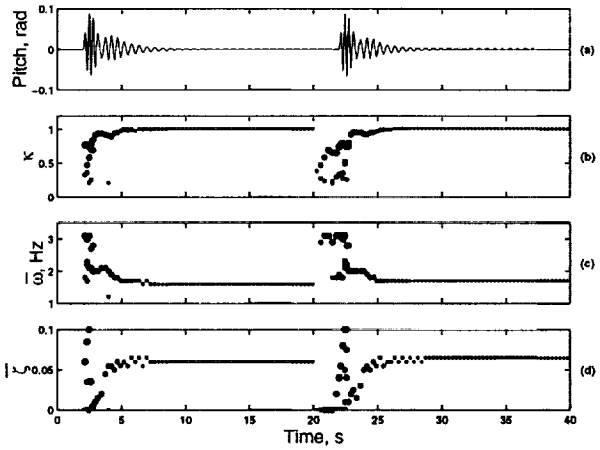

Figure 9: Correlation Filtering of the Nonlinear Simulation Response with the Laplace Wavelet Dictionary Ψ : Pitch State Variable (a), Correlation Coefficient κ (b), Wavelet Frequency $\overline{\omega}$ Associated with Peaks of κ (c), Wavelet Damping $\overline{\zeta}$ Associated with Peaks of κ (d)

Figure 9a presents the time history of the nonlinear simulation. Figures 9b, 9c, and 9d present the resulting correlation coefficient, frequency values, and damping values respectively. For each decay, inspection of the correlation coefficient κ clearly indicate regions of linear and nonlinear behavior. Nonlinear behavior occurs at higher amplitudes in the first 2 s of each decay and then transitions to behavior characteristic of a linear time invariant system. This behavior is indicated in Figures 9b through 9d. The nonlinear region is marked by lower correlation values, a decreasing frequency trend characteristic of hardening springs, and a certain amount of data scatter. This scatter disappears as κ increases to unity, and the frequency values $\overline{\omega}$ and damping values $\overline{\zeta}$ converge on constants. These constants are the wavelet parameters nearest the corresponding linearized system characteristics for ω_α and ζ_α given in Table 3. This analysis confirms the Laplace wavelet correlation analysis properly identifies linearized dynamics for nonlinear systems operating in their linear range.

Experimental data from nonlinear systems can now be analyzed in this fashion. Measurements of the wing movement are recorded at different airspeeds to analyze dynamical properties of the nonlinear system.

A series of measurements are made by releasing the wing from an initial plunge displacement ($0.02m$) and recording until the motion essentially stops, with the process repeated by increasing the airspeed and releasing the wing after resetting the position to the desired initial conditions. Correlation filtering of these responses for airspeeds $U = 6, 8\ m/s$ using a minimum threshold $\kappa_{min} = .2$ results in the information shown in Figure 10.

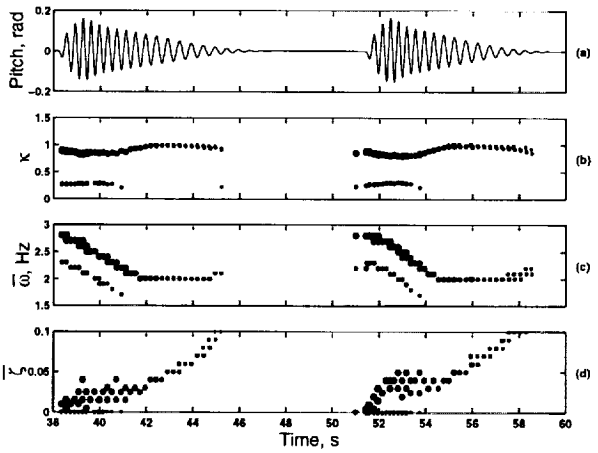

Figure 10: Correlation Filtering of the Texas A&M University Nonlinear Testbed with the Laplace Wavelet Dictionary Ψ : Pitch Measurement (a), Correlation Coefficient κ (b), Wavelet Frequency $\bar{\omega}$ Associated with Peaks of κ (c), Wavelet Damping $\bar{\zeta}$ Associated with Peaks of κ (d)

A visual inspection of the pitch angle measurements in Figure 10a can identify several features of the response associated with the nonlinear hardening spring. The initial local frequency decreases after 2 s when the response decays to small angles. Also, the plunge motion, which is not displayed in the Figure, decays quickly during the initial 2 s so the response is dominated by the mode associated with pitch motion.

The correlation coefficient κ shown in Figure 10b indicates the Laplace wavelets have good similarity to the initial response but have a stronger similarity to the decaying response at smaller amplitudes. This time-varying correlation is intuitive since the wavelet is derived to match the response from a linear system and the wind tunnel system is strongly nonlinear initially but nearly linear when the pitch angle decays to small values. The additional set of correlation coefficients below $\kappa \approx .3$ are believed to be related to the plunge motion of the wing and corresponds to the second frequency seen in Figure 10c.

The wavelet frequency $\bar{\omega}$ quantifies the time-varying local frequency which is expected for the response of a hardening spring. The initial frequency is high but decreases steadily as the transient response decays until α is small and the system behaves like a linear system. The final value of $\bar{\omega}$ when $\kappa \approx 1$ is approximately 20 percent higher than the predicted frequency from Table 3. This identifies errors in the model relative to the particular experimental configuration being investigated here.

The wavelet damping $\bar{\zeta}$ in Figure 10d varies with time. The scatter is reduced when κ and $\bar{\omega}$ are constant but never settles on a clear damping value which can be easily extracted. This behavior may be reasonable for highly nonlinear systems. However, the corresponding high correlation values at lower amplitudes suggests confidence in the damping estimates, so a nonviscous damping mechanism such as coulomb damping may be occurring. This idea is supported by inspection of Figure 10a which indicates a linear rather than an exponential amplitude envelope.

A series of these responses are measured at incrementally increasing airspeeds including the unstable airspeeds at which limit cycle oscillations occur. Figure 11 presents the response measurements and airspeeds along with damping and frequency information obtained from the correlation filtering.

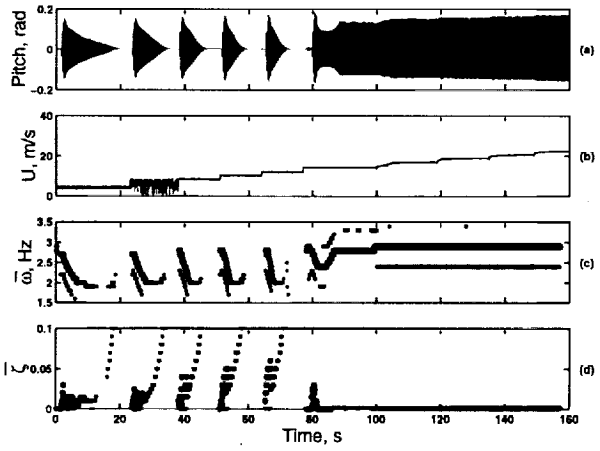

Figure 11: Correlation Filtering of the Texas A&M University Nonlinear Testbed with the Laplace Wavelet Dictionary Ψ : Pitch Measurement (a), Airspeed (b), Wavelet Frequency $\bar{\omega}$ Associated with Peaks of κ (c), Wavelet Damping $\bar{\zeta}$ Associated with Peaks of κ (d)

Figure 11 emphasizes that the features observed in Figure 10 extend across a wide range of velocities. The frequency and damping demonstrate the same time-varying behavior for each airspeed below the instability at $U = 13.5\ m/s$, characterized by decreasing $\bar{\omega}$ and increasing $\bar{\zeta}$ as the response decays. Also, ψ_γ for two frequencies have high correlation to the limit cycle responses at velocities beyond $U = 13.5\ m/s$.

The rate of time variation for $\bar{\zeta}$ is suggestive of the relationship between system dynamics and the wavelet support range. The response decays faster at higher

airspeeds so the system quickly approximates linear dynamics and quickly decays to below the correlation threshold. The wavelet dictionary does not compensate for this increased decay rate so the support range, which is good at low airspeeds, becomes less effective as airspeed increases. Information about the system damping is particularly difficult to obtain from correlation filtering of the response at the last stable test point $U = 12\ m/s$.

8. Conclusions

The Laplace wavelet is a useful waveform for analysis of transient signals due to its formulation as an impulse response of an underdamped second order system. The inherent properties of this waveform can be interpreted as traditional modal analysis concepts such as damped natural frequency and viscous damping ratio. A method of correlation filtering is introduced based on a dictionary of Laplace wavelets that correlates a measured response with wavelets of different frequencies and dampings. Identifying the wavelets which correlated highly with the signal indicates the modal properties of the system which generated that signal. Modal properties of aeroelastic systems are identified using this correlation filtering approach.

Analysis of aircraft flight flutter test data resulted in estimates of frequency and damping versus time, with a measure of relative confidence in those estimates. These estimates correctly indicated a trend toward an instability which actually occurred. The linearized dynamics of a nonlinear wind tunnel system are also identified until a bifurcation induces a limit cycle oscillation.

9. Acknowledgements

Rick Lind was supported by a NASA-National Research Council Postdoctoral Fellowship. Early concepts for applying wavelets to structural dynamic problems were developed with Ronald Nelson through the NASA-JOVE program and Sydney Haley through the NASA Co-op program. The wind tunnel data was acquired by David Thompson through NASA Cooperative Agreement No. NCC4-111.

References

[1] Bennett, R. and Abel, I., "Application of a Flight Test and Data Analysis Technique to Flutter of a Drone Aircraft," *AIAA Structures, Structural Dynamics and Materials Conference*, Atlanta GA, AIAA-81-0652, April 1981.

[2] Brenner, M., Lind, R. and Voracek, D., "Overview of Recent Flight Flutter Testing Research at NASA Dryden," *AIAA Structures, Structural Dynamics, and Materials Conference*, Orlando FL, AIAA-97-1023, April 1997.

[3] Dowell, E., "Nonlinear Aeroelasticity," *AIAA Structures, Structural Dynamics, and Materials Conference*, Long Beach CA, April 1990, AIAA-90-1031, pp. 1497-1509.

[4] Gilliat, H., Strganac, T., and Kurdila, A. "Nonlinear Aeroelastic Response of an Airfoil," *AIAA Aerospace Sciences Meeting*, Reno NV, AIAA-97-0459, January 1997.

[5] Gilyard, G. and Edwards, J. *Real-time Flutter Analysis of an Active Flutter Suppression System on a Remotely Piloted Research Aircraft*, NASA-TM-84901, January 1983.

[6] Kailath, T., *Linear Systems*, Prentice-Hall, Englewood Cliffs, NJ, 1980.

[7] Kehoe, M., "A Historical Overview of Flight Flutter Testing," 80^{th} *AGARD Structures and Materials Panel*, AGARD-CP-566, Rotterdam, The Netherlands, May 8-10 1995, pp. 1-15.

[8] Lind, R., Brenner, M., and Haley, S., "Estimation of Modal Parameters Using a Wavelet-Based Approach," *AIAA Atmospheric Flight Mechanics Conference*, New Orleans LA, AIAA-97-3836, August 1997.

[9] Mallat, S. and Zhang, Z., "Matching Pursuit with Time-Frequency Dictionaries," *IEEE Transactions on Signal Processing*, Vol. 41, No. 12, December 1993, pp. 3397-3415.

[10] Newsom, J. and Pototzky, A., "Comparison of Analysis and Flight Test Data for a Drone Aircraft with Active Flutter Suppression," *AIAA Structures, Structural Dynamics and Materials Conference*, Atlanta GA, AIAA-81-0640, April 1981.

[11] O'Neil, T., Gilliat, H., and Strganac, T., "Investigations of Aeroelastic Response for a System with Continuous Structural Nonlinearities," *AIAA Structures, Structural Dynamics, and Materials Conference*, Salt Lake City UH, AIAA-96-1390, April 1996.

[12] Shelley, S., Freudinger, L., and Allemang, R., "Development of an On-Line Parameter Estimation System Using the Discrete Modal Filter," *International Modal Analysis Conference*, San Diego, CA, February 1992, pp. 173-183.

[13] Shelley, S. and Pickrel, C., "New Concepts for Flight Flutter Parameter Estimation," *International Modal Analysis Conference*, Orlando FL, February 1997, pp. 490-496.

[14] Strang, G. and Nguyen, T., *Wavelets and Filter Banks*, Wellesley-Cambridge Press, 1996.